Leveraging 3D Geometric Priors in 2D Rotation Symmetry Detection
— Supplemental Material —

A.1. Use of Estimated Camera Intrinsics

In the main paper, we used a fixed focal length of 1000 due to missing camera intrinsics. To improve this, we apply DiffCalib[1], a diffusion-based model that estimates intrinsics from monocular images. Using DiffCalib, we estimate focal lengths for each DENDI image. These values vary widely, as shown in Fig. a.1, so we clip the normalized focal lengths to the range $[2/3, 4/3]$ for training stability. Our original 3D model used a fixed point cloud range of $[-1, 1]$ m (x-y) and $[0, 4]$ m (z). To accommodate the variation in focal lengths, we expand this range by a factor of 4.

Results in Tab. a.1 show that our model achieves 20.5 mAP with 800 scores (same as the main paper), and improves to 25.0 mAP with 3200 scores—the highest among all settings. Although this is lower than the 30.6 mAP in Table 4, the drop is due to unstable intrinsics and unoptimized hyperparameters. Still, our vertex reconstruction consistently outperforms the 3D baseline in all cases.

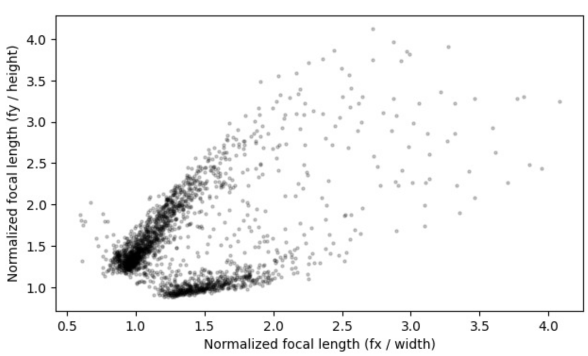

Figure a.1. Normalized focal length distribution of DENDI.

A.2. Analysis in 3D

To analyze the effectiveness of incorporating explicit 3D geometric priors for rotation symmetry detection, we established a 3D baseline model that predicts 3D points and projects them into 2D image space. The qualitative results in Fig. a.2 showcase four samples from the DENDI validation and test sets, arranged in rows, each containing six items. In each row, four images (input image, ground truth, 2D baseline, 3D baseline, and ours) are displayed in a 2x2 format, with two plots on the right.

The accompanying plots visualize the 3D predicted points from the 3D baseline and our method in XYZ camera coordinates. Key points include the rotation center (red dot) and rotation vertices (blue dots). Additionally, triangles formed by the center and two nearby vertices are illustrated, providing insight into the 3D placement of the points, including distances and co-planarity, highlighting the geometric accuracy of our approach.

In row (a), showing a C_4 object, all models detect the correct vertices, but ours achieves the best localization. The 3D baseline appears accurate in 2D but fails to maintain correct 3D geometry, highlighting the benefit of our geometric priors. In row (b), with C_8 and C_2 signs, our method performs best on the octagon but lags slightly on C_2 compared to the 2D baseline—likely due to the simpler nature of bounding box detection and our still-developing C_2 reconstruction. Overall, our method improves 2D accuracy by enforcing 3D geometric constraints.

Table a.1. Rotation vertex detection results on DENDI *test*.

Method	3D model	3D prior	mAP_{800}	mAP_{3200}
2D Baseline			22.6	23.1
3D Baseline	✓		14.8	15.8
Ours	✓	✓	20.5	25.0

A.3. Additional Qualitative Results

Fig. a.3 shows additional qualitative comparisons between the 2D baseline, 3D baseline, and our method. The results demonstrate that our model effectively detects dense rotational symmetries in real-world scenes. By incorporating 3D geometric priors, our method improves localization in the 3D detection setting. Notably, in the fourth row, it outperforms both baselines on objects with C_5 symmetry.

[1]He, Xiankang, et al. "DiffCalib: Reformulating Monocular Camera Calibration as Diffusion-Based Dense Incident Map Generation." *arXiv preprint*, 2024.

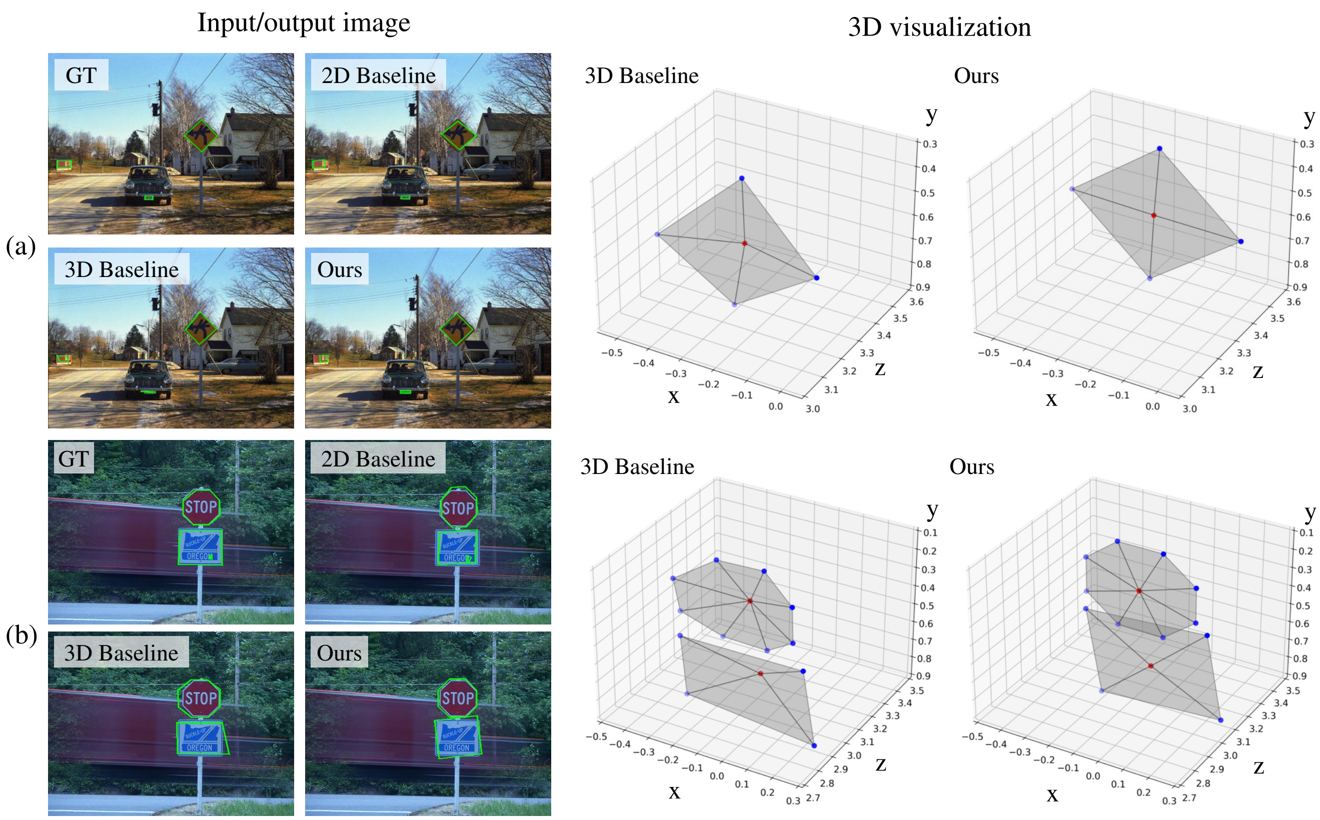

Figure a.2. **Qualitative comparison of rotation vertex detection results on the DENDI dataset.** Each row displays input images with detected vertices (true positives in green, others in cyan) for the ground truth, 2D baseline, 3D baseline, and our method, alongside 3D plots visualizing the predicted points and geometric properties such as distances and co-planarity.

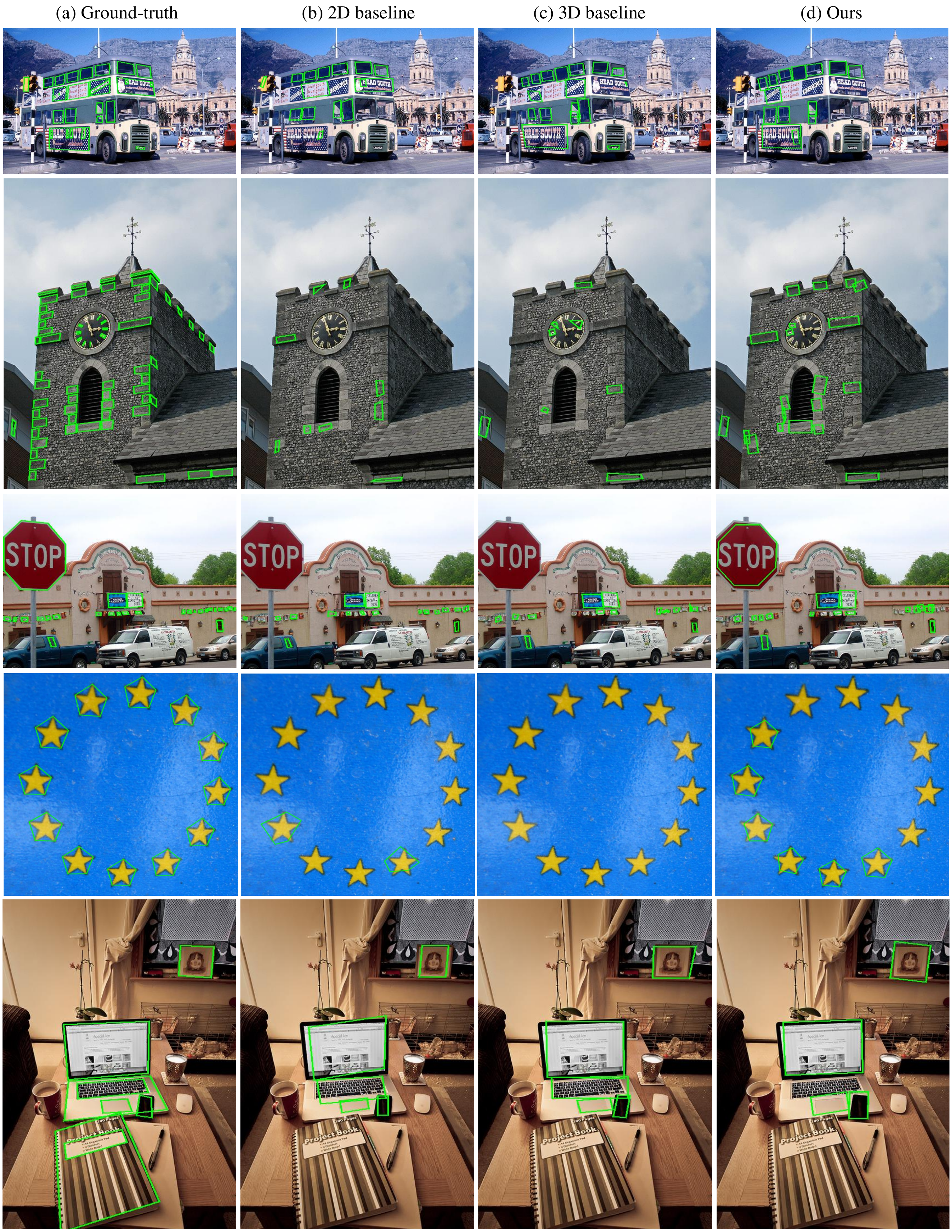

Figure a.3. **Qualitative comparison of rotation vertex detection results on the DENDI dataset.** Each set of four columns displays the ground truth, the 2D baseline, the 3D baseline, and ours. True-positive polygons are marked in green; otherwise, they are marked in cyan.